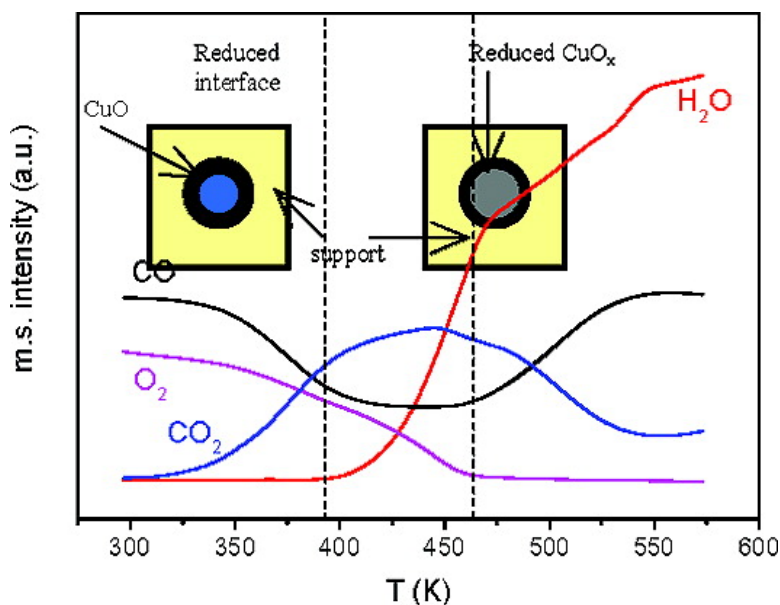


Selective CO Oxidation in Excess H over Copper–Ceria Catalysts: Identification of Active Entities/Species

Daniel Gamarra, Carolina Belver, Marcos Fernandez-Garca, and Arturo Martinez-Arias

J. Am. Chem. Soc., **2007**, 129 (40), 12064-12065 • DOI: 10.1021/ja073926g • Publication Date (Web): 18 September 2007

Downloaded from <http://pubs.acs.org> on February 14, 2009



More About This Article

Additional resources and features associated with this article are available within the HTML version:

- Supporting Information
- Links to the 2 articles that cite this article, as of the time of this article download
- Access to high resolution figures
- Links to articles and content related to this article
- Copyright permission to reproduce figures and/or text from this article

[View the Full Text HTML](#)

Selective CO Oxidation in Excess H₂ over Copper–Ceria Catalysts: Identification of Active Entities/Species

Daniel Gamarra, Carolina Belver, Marcos Fernández-García, and Arturo Martínez-Arias*

Instituto de Catálisis y Petroleoquímica, CSIC, C/Marie Curie 2, Campus de Cantoblanco, 28049 Madrid, Spain

Received May 31, 2007; E-mail: amartinez@icp.csic.es

Production of H₂ for polymer fuel cells (PEMFC) is usually accomplished by a multistep process that includes catalytic reforming of hydrocarbons followed by water gas shift (WGS).^{1,2} However, due to the limited activities of the current WGS catalysts, approximately 0.5–1.0 vol % of unconverted CO still remains in the effluent and needs to be decreased to a trace level to avoid poisoning of the PEMFC anode.³ Preferential oxidation of CO in the H₂-rich stream resulting from such processes (CO-PROX) has been recognized as one of the most straightforward and cost-effective methods to achieve acceptable CO concentrations (below ca. 100 ppm).^{4–6} Supported noble metal catalysts, in particular, those containing platinum or gold,^{4–8} have shown their ability for the process, and commercial systems based on supported platinum are available.^{3,9} Catalysts based on combinations between copper and cerium oxides have also shown promising properties for the process and constitute a more interesting alternative from an economical point of view.^{4,10,11} It is generally agreed that optimum catalytic properties for CO oxidation over copper–ceria are achieved in the presence of well-dispersed copper oxide patches over ceria nanoparticles.^{4,10–12} However, fundamental questions remain unanswered regarding the nature of the active species or sites for the two competing CO and H₂ oxidation reactions whose respective activities determine the selectivity behavior of the catalyst. The present work shows, on the basis of *Operando* spectroscopic analyses, that the CO-PROX performance of these types of catalysts could be modulated since the two oxidation reactions are apparently favored by different redox processes involving the copper oxide support interface (for CO oxidation) and propagation of the reduction to the rest of the supported copper oxide particles (for H₂ oxidation).

A catalyst with ca. 5 wt % of copper oxide supported on ceria (5CuO/CeO₂) was prepared by incipient wetness impregnation of copper nitrate on a nanocrystalline CeO₂ support prepared by a microemulsion method. A copper–cerium mixed oxide catalyst (Cu_{0.2}Ce_{0.8}O₂) was prepared by coprecipitation of copper and cerium within a reverse microemulsion. Calcination under air at 773 K was applied as the final step of the preparation in any case. A multitechnique analysis detailing structural and electronic characteristics of these catalysts can be found elsewhere.^{11,13}

Comparing these two catalysts, a previous work reported higher CO and H₂ oxidation activity under CO-PROX conditions over Cu_{0.2}Ce_{0.8}O₂ during experiments conducted in a tubular fixed bed catalytic reactor in which full CO conversion was achieved in a narrow window for both catalysts; nevertheless, 5CuO/CeO₂ displayed slightly higher overall selectivity for CO oxidation.¹¹ Similar results are observed in the activity tests carried out with the DRIFTS cell (Supporting Information). The DRIFTS spectra (Supporting Information) display the formation of different carbonate-type species on the catalysts already upon first contact with the CO-PROX mixture at 303 K. Similar carbonates are detected on the CeO₂ support, although they appear at considerably higher reaction temperature (see Supporting Information). This indicates

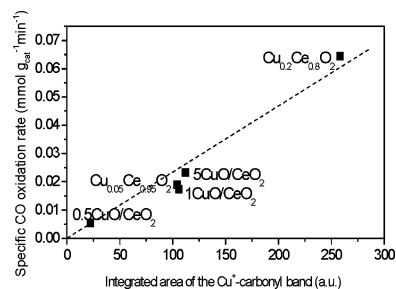


Figure 1. CO oxidation rate at 323 K as a function of the intensity of the Cu⁺ carbonyl calculated just prior to CO oxidation onset for the indicated catalysts. The analysis is extended to copper–ceria systems whose characteristics can be found elsewhere.¹¹

that the interfacial region of the support in contact with the dispersed copper oxide entities remains carbonated during the course of the reaction as a consequence of the strongest redox activity of such region which should facilitate carbonate formation.¹⁴ This must be taken into account when considering possible redox equilibrium between copper and cerium at the interfacial region.¹⁰

Additionally, a band at 2120–2110 cm⁻¹ appears upon interaction with the CO-PROX mixture already at 303 K (Supporting Information). Interestingly, a correlation is found between the intensity of this band and the CO oxidation activity of the catalysts, as displayed in Figure 1. It must be noted that, although the frequency of this band lies in the range expected for metallic copper carbonyls,¹⁵ their relatively large thermal stability, along with previous analysis of the redox properties of these catalysts, indicates that they must correspond to Cu⁺-carbonyls affected by interactions with the support and therefore located at interfacial positions of the dispersed copper oxide entities.^{11,14,16} The correlation illustrated by Figure 1 can be understood on the basis of a recent analysis of redox properties of this type of catalysts under CO/O₂ and considering the Mars–van Krevelen-type mechanism under which CO oxidation apparently proceeds in these types of catalysts.^{10,14} In this sense, taking into account the fully oxidized initial state of the catalysts,^{11,13} the respective intensities of these Cu⁺-carbonyls provide a measure of the potential of each catalyst to become interfacially reduced (within the Cu²⁺/Cu⁺ redox couple)¹⁴ upon interaction of CO with its dispersed copper oxide entities, whereas the level of reduction attained in each case is in turn related to the amount of sites available for oxygen to react and close the catalytic cycle.^{10,14}

These results are complemented by XANES under CO-PROX conditions. The analysis of the Cu *K*-edge XANES spectra of Cu_{0.2}Ce_{0.8}O₂ and 5CuO/CeO₂ indicates the presence of three different chemical species during the course of the runs (Supporting Information).¹⁷ The first one corresponds to a Cu²⁺ chemical state displaying geometry similar to that found in CuO although displaying some particularities attributable to interactions with the support, as discussed in more detail elsewhere.^{13,14} This component predominates at low reaction temperature, as illustrated by Figure

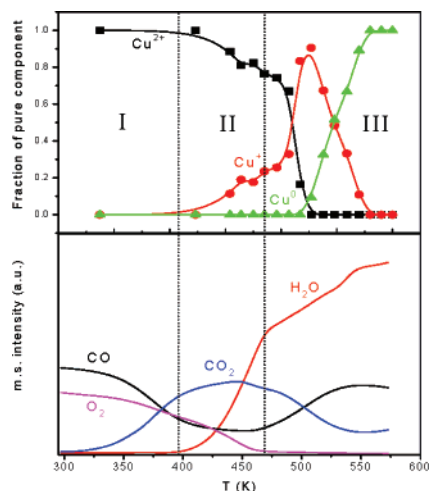


Figure 2. Evolution of principal components detected by XANES during a CO-PROX test over $\text{Cu}_{0.2}\text{Ce}_{0.8}\text{O}_2$ and evolution of the gases during the same run.

2. In this sense, it must be noted that the level of copper reduction evidenced by DRIFTS at low temperature must correspond to a relatively low amount of the copper (note a maximal limit of ca. 10% as intrinsic error of the technique/analysis), exclusively related to interfacial sites in close interaction with the support which presents the highest redox activity.¹⁴ A component corresponding to zero-valent Cu^0 , as identified from comparison with a Cu foil reference, predominates at the end of the runs (Figure 2). An intermediate species is detected during spectra analysis and attributed to a Cu^+ state on the basis of its $1s \rightarrow 4p/3d$ transition energy and spectral shape (see Supporting Information).¹³ Joint analysis of the evolutions of the various copper species and the gases evolving during the CO-PROX tests allows separation of different relevant zones (Figure 2). The first one (zone I) at lowest reaction temperature involves basically CO oxidation and has been discussed above on the basis of DRIFTS experiments. The second zone (II) displays a correlation between onset of H_2 oxidation and, at slightly lower temperature, onset of massive copper reduction to Cu^+ . This correlation indicates the involvement of the latter species in H_2 oxidation, in agreement with the high reactivity shown by partially reduced copper oxide toward hydrogen.¹⁸ Note that, as a difference with CO oxidation, H_2 oxidation takes place when the reduction is propagated to zones of the copper oxide nanoparticles not strictly in direct contact with the support. In this respect, H_2 oxidation can be most dependent on the specific properties (size, shape)¹⁹ of the dispersed copper oxide nanoparticles, as pointed out previously.¹² In contrast, CO oxidation properties are most likely governed by the characteristics of the CuO-support contacts, i.e., the interfacial properties.¹⁴ A third zone (III) is detected at higher temperature during H_2 oxidation in which the reaction rate changes in coincidence with a sharp increase of the Cu^+ contribution. This can be related to the formation of less active Cu_2O or to sintering of the copper prior to generation of metallic copper.^{14,18} This is detected at the highest reaction temperature, and its formation fairly coincides with appearance of Ce^{3+} (see analysis of the Ce L_{III} zone in Supporting Information). Certainly, the copper segregation produced by this reduction process can contribute to the small deactivation observed in these types of systems when maintained under the reactant mixture at relatively high temperature.^{20,21} Validation of the correlations observed for $\text{Cu}_{0.2}\text{Ce}_{0.8}\text{O}_2$ is provided by observation of similar ones for $5\text{CuO}/\text{CeO}_2$ (Supporting Information).

Concerning the type of oxygen species that could be involved in the reaction mechanism, Raman spectra recorded under reaction

conditions for $\text{Cu}_{0.2}\text{Ce}_{0.8}\text{O}_2$ did not show the formation of peroxide or superoxide species under CO-PROX conditions (Supporting Information). Such species were proposed to be involved during CO-PROX processes in ceria-supported gold systems.⁸ Their absence in $\text{Cu}_{0.2}\text{Ce}_{0.8}\text{O}_2$ suggests that oxygen species involved in the redox processes can be directly oxide anions, in agreement with a recent investigation in which redox changes under CO/O_2 in a catalyst of this type were observed to occur without involvement of superoxides or peroxides even at 303 K,²² at which they can be stable.¹⁴

In summary, DRIFTS and XANES results allow analyzing the entities/species and/or phenomena involved in the two (CO and H_2) oxidation reactions taking place during CO-PROX tests over the catalysts. They demonstrate that CO oxidation takes place at interfacial positions of the dispersed copper oxide entities, and a correlation is established between such activity and the level of reduction achieved in such entities. The H_2 oxidation is shown to proceed immediately after onset of a massive copper reduction to Cu^+ , indicating that active species for the process must be mainly related to partially reduced dispersed copper oxide nanoparticles. Copper segregation and formation of metallic copper occurs at $T > \text{ca. } 473 \text{ K}$ and can contribute to the partial deactivation observed for these types of systems under the CO-PROX mixture.²¹

Acknowledgment. D.G. and C.B. thank the FPI and Juan de la Cierva MEC programs, respectively. The help provided by Dr. S.G. Fiddy at SRS station 7.1 (project # 44072) during recording of XANES spectra is greatly acknowledged. Financial support by Comunidad de Madrid (ENERCAM S-0505/ENE/000304) and MEC (CTQ2006-15600/BQU) is acknowledged.

Supporting Information Available: Experimental procedure, *Operando* DRIFTS and XANES results, and in situ Raman spectra. This material is available free of charge via the Internet at <http://pubs.acs.org>.

References

- Rostrup-Nielsen, J. R.; Sehested, J.; Nørskov, J. K. *Adv. Catal.* **2002**, *47*, 65.
- Fu, Q.; Saltsburg, H.; Flytzani-Stephanopoulos, M. *Science* **2003**, *301*, 935.
- Ghenciu, A. F. *Curr. Opin. Solid State Mater. Sci.* **2002**, *6*, 389.
- Avgouropoulos, G.; Ioannides, T.; Papadopoulou, Ch.; Batista, J.; Hocevar, S.; Matralis, H. K. *Catal. Today* **2002**, *75*, 157.
- Kahllich, M. J.; Gasteiger, H. A.; Behm, R. J. *J. Catal.* **1997**, *171*, 93.
- Ko, E.-Y.; Park, E. D.; Lee, H. C.; Lee, D.; Kim, S. *Angew. Chem., Int. Ed.* **2007**, *46*, 734.
- Griessel, R. J. H.; Weststrate, C. J.; Goossens, A.; Craje, M. W. J.; van der Kraan, A. M.; Nieuwenhuys, B. E. *Catal. Today* **2002**, *72*, 123.
- Guzman, J.; Carrettin, S.; Corma, A. *J. Am. Chem. Soc.* **2005**, *127*, 3286.
- Farrauto, R.; Hwang, S.; Shore, L.; Ruettinger, W.; Lampert, J.; Giroux, T.; Liu, Y.; Ilinich, O. *Annu. Rev. Mater. Res.* **2003**, *33*, 1.
- Sedmak, G.; Hocevar, S.; Levec, J. *J. Catal.* **2003**, *213*, 135.
- Gamarra, D.; Munuera, G.; Hungria, A. B.; Fernández-García, M.; Conesa, J. C.; Midgeley, P. A.; Wang, X. Q.; Hanson, J. C.; Rodríguez, J. A.; Martínez-Arias, A. *J. Phys. Chem. C* **2007**, *111*, 11026.
- Martínez-Arias, A.; Hungria, A. B.; Fernández-García, M.; Conesa, J. C.; Munuera, G. *J. Power Sources* **2005**, *151*, 32.
- Wang, X. Q.; Rodríguez, J. A.; Hanson, J. C.; Gamarra, D.; Martínez-Arias, A.; Fernández-García, M. *J. Phys. Chem. B* **2005**, *109*, 19595.
- Martínez-Arias, A.; Hungria, A. B.; Fernández-García, M.; Conesa, J. C.; Munuera, G. *J. Phys. Chem. B* **2004**, *108*, 17983.
- Hollins, P. *Surf. Sci. Rep.* **1992**, *16*, 51.
- Martínez-Arias, A.; Fernández-García, M.; Gálvez, O.; Coronado, J. M.; Anderson, J. A.; Conesa, J. C.; Soria, J.; Munuera, G. *J. Catal.* **2000**, *195*, 207.
- Fernández-García, M. *Catal. Rev. Sci. Eng.* **2002**, *44*, 59.
- Kim, J. Y.; Rodríguez, J. A.; Hanson, J. C.; Frenkel, A. I.; Lee, P. L. *J. Am. Chem. Soc.* **2003**, *125*, 10684.
- Fernández-García, M.; Martínez-Arias, A.; Hanson, J. C.; Rodríguez, J. A. *Chem. Rev.* **2004**, *104*, 4063.
- Kim, D. H.; Cha, J. E. *Catal. Lett.* **2003**, *86*, 107.
- Martínez-Arias, A.; Hungria, A. B.; Munuera, G.; Gamarra, D. *Appl. Catal. B* **2006**, *65*, 207.
- Martínez-Arias, A.; Gamarra, D.; Fernández-García, M.; Wang, X. Q.; Hanson, J. C.; Rodríguez, J. A. *J. Catal.* **2006**, *240*, 1.

JA073926G